Scheimpflug imaging: Optical distortion correction

3

3. Scheimpflug imaging: Optical distortion correction

The contribution of Patricia Rosales to this study was the implementation of optical distortion correction algorithms, particularly adapting them to the Scheimpflug system available in the laboratory (Pentacam, Oculus), development of a method to infere the camera nodal points and tests on artificial eyes of known dimensions and on a normal eye. Previous experience and suggestions from Michael Dubbelman and Rob van der Heijde who had developed optical distortion correction algorithms on other Scheimpflug systems have been essential. Suggestions from Susana Marcos, Alberto de Castro, Lucie Sawides, Alfonso Fernandez Escudero and Carlos Dorronsoro have been very valuable in important points to develop the algorithms.

RESUMEN

Objetivos: Desarrollar algoritmos de corrección para la cámara comercial de Scheimpflug Pentacam, Oculus.

Métodos: Para la obtención del punto nodal de la cámara se tomaron imágenes de esferas calibradas de radios conocidos: 9.65 mm, 8 mm y 6 mm, y una imagen de un papel milimetrado. Mediante funciones de minimización, se fue variando la posición del punto nodal, hasta que el radio proyectado en el plano objeto coincidía con los radios nominales de las esferas. Una vez hallados los puntos nodales, se aplicaron los algoritmos de corrección de la distorsión sobre imágenes de un ojo artificial de dimensiones conocidas y un ojo normal medido anteriormente con una cámara de Scheimpflug con la distorsión óptica corregida (Topcon SL-45, Vrije University, Amsterdam, The Netherlands).

Resultados: Los puntos nodales obtenidos recuperan el radio nominal de la esfera calibrada al 100% y la distancia entre dos puntos consecutivos del papel milimetrado con una precisión del 95%. Los radios de curvatura de las superficies oculares de las imágenes sin corregir eran mayores que las de las imágenes corregidas. El error promedio en la recuperación de los radios de curvatura nominales fue de 0.18 mm y 0.27 mm para las caras anterior y posterior de la córnea y de 0.37 y 0.46 mm para las caras anterior y posterior del cristalino. El error promedio cometido al recuperar las distancias intraoculares fue de 0.015mm, 0.385mm y 0.048 mm para el espesor de la córnea, la cámara anterior y el espesor del cristalino respectivamente.

Conclusiones: Los resultados sugieren que los algoritmos corrigen con bastante precisión las distorsiones geométrica y óptica de la cámara de Scheimpflug. Sin embargo, el conocimiento exacto de los puntos nodales de la cámara (ahora estimado mediante un método de mínimos cuadrados) mejoraría la precisión del método.

ABSTRACT

Purpose: To develop algorithms for the optical and geometrical distortion correction of the commercial Scheimpflug camera Pentacam, Oculus.

Methods: To obtain the camera nodal points, images of calibrated espheres and an image of millimetre paper were obtained with the Scheimpflug camera. The radius of those spheres were of 9.65, 8 and 6 mm. Using a merit function and a least-mean square procedure, several nodal point positions were tested, until the projected radius on the object plane matched the nominal radius values of the espheres. Once the nodal points were obtained, the correction distortion algorithms were applied on Scheimpflug images of an artificial eye with known dimensions and images of a normal eye previously measured with an optical and geometrical distortion corrected Scheimpflug camera (Topcon SL-45, from the Vrije University, Amsterdam, Holland).

Results: The estimated nodal points allowed to obtain the nominal radius of the calibrated ball with an accuracy of 100%, and distances in the images with an accuracy of 95%. The radius of curvature of the ocular surfaces of the uncorrected surfaces were higher than the corrected images. The average error in the retrieved radius of curvature were of 0.18 and 0.27 mm for the anterior and posterior cornea radius of curvature respectively, and of 0.37 and 0.46 mm for the anterior and posterior crystalline lens radius of curvature respectively. The average error in the retrieved intraocular distances were of 0.015mm, 0.385 mm and 0.048 mm for corneal thickness, anterior chamber depth and lens thickness respectively.

Conclusions: The results suggest that the distortion correction algorithms are quite accurate, although inaccuracies to retrieve the nominal radius of curvature and intraocular distances, can be minimized by a more precise knowledge of the nodal points.

1. INTRODUCTION

Scheimpflug imaging is a powerful tool for anterior segment imaging, but special care must be taken in correcting the images for the geometrical distortion (caused by the tilt of the object plane with respect to the optical axis) and for the optical distortion (caused by refraction from the different ocular surfaces, i.e, the posterior cornea is seen refracted from anterior cornea, anterior crystalline lens is seen refracted by posterior and anterior cornea, and posterior crystalline lens is seen refracted by anterior crystalline lens and anterior and posterior cornea).

The first Scheimpflug imaging set up systematically used in the lab for investigation of the crystalline lens was developed by Brown (Brown, 1973, Brown, 1974). While these authors did introduce corrections for the geometrical distortion, the optical distortion did not seem to be fully corrected. Brown's study reports a decrease of the anterior and posterior lens radius of curvature with age (Brown, 1974). More recent studies also show a decrease in the anterior and posterior lens radii of curvature with age, but to a lesser extent. Whereas Brown found a decrease in the anterior lens radius of curvature of 100 μm/year. Dubbelman (Dubbelman & van der Heijde, 2001), using a distortion corrected Scheimpflug camera found a decrease of 57 μm/year, while findings for the posterior lens radius of curvature are similar for both authors. Dubbelman also found smaller values for the absolute value for the anterior and posterior lens radius of curvature.

Different methods have been applied in order to correct for the optical distortion. Cook (Cook & Koretz, 1998) proposed a method based on a Hough transform in order to obtain corrected surfaces from Scheimpflug images. This method has been validated through comparison with MRI (Koretz, Strenk, Strenk & Semmlow, 2004) but on a different set of subjects.

Dubbelman (Dubbelman & van der Heijde, 2001, Dubbelman, van der Heijde & Weeber, 2001) have conducted thorough developments of correcting algorithms and validations on refurbished prototypes of the Topcon SL-45 and Nidek Eas-1000 systems. These systems were developed in the 80’s and 90’s respectively, and were commercially available for some time, although both are now discontinued. Figure 3.1 and 3.2 show the optical configuration of both systems. Some of the hardware modifications in the systems performed by Dubbelman and collegues include the

replacement of the original camera by high-resolution scientific grade CCD cameras. In both cases, images are taken along one meridian, which can be manually changed of orientation. Typically, data are obtained on the horizontal and vertical meridians. The geometrical distortion in this system is corrected by projecting the CCD chip from the image plane to the object plane passing through the nodal points. The optical distortion is corrected by means of ray tracing. The anterior surface of the cornea only suffers from geometrical distortion. Tracing this surface back from the image plane (CCD-chip) through the optics of the camera (with the critical dimensions of the optical layout being provided by the manufacturer) to the object plane (slit beam) gives the corrected anterior corneal surface. The posterior corneal surface is traced through the nodal point and the anterior cornea to obtain the undistorted coordinates of the posterior corneal surface on the object plane. The anterior surface of the lens is then traced through the nodal points and the anterior and posterior corneal surfaces. A similar procedure is followed for the posterior lens surface.

Figure 3.3 shows an example of a typical raw image obtained with the Topcon SL system in a young (16 years old) dilated human eye, and after correction for geometrical and optical distortion. Measurements on an artificial eye (Dubbelman & van der Heijde, 2001) show differences between corrected and uncorrected images that can be summarized in Table 3.1.

Table 3.1. Radius of curvature and thickness of both elements of the artificial eye. (Dubbelman & van der Heijde, 2001).

	Nominal Values	Before correction	After correction
Anterior cornea	8.9 ± 0.05	9.34±0.08	8.93±0.08
Posterior cornea	8.29± 0.05	9.17±0.08	8.27±0.12
Cornea thickness	0.501±0.001	0.28±0.02	0.50±0.02
Anterior lens	13.07±0.05	15±1.1	13.0±0.16
Posterior lens	13.06±0.05	26±2.8	12.29±
Lens thickness	4.285±0.001	4.0±0.14	4.24±0.06

The Scheimpflug imaging phakometry data presented in Chapter 4 of this thesis was performed using a Topcon SL-45 system, with correcting algorithms developed by Dubbelman (Dubbelman, van der Heijde & Weeber, 2005) .

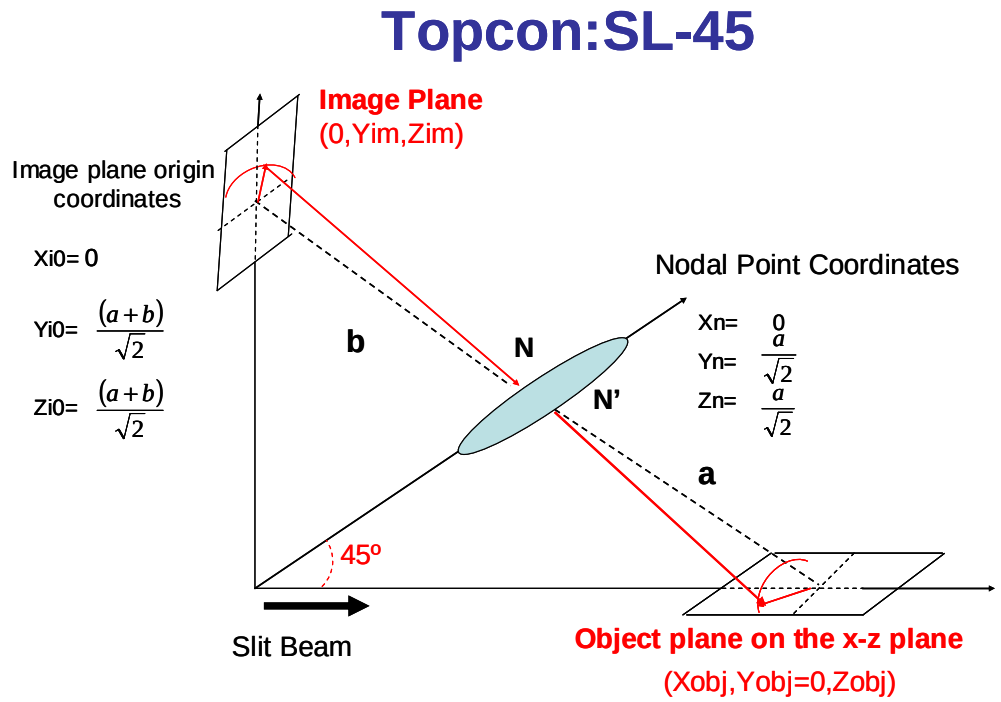

Figure 3.1. Configuration of the Scheimpflug camera Topcon SL-45. The image plane and the object plane (the anterior segment of the eye) form an angle of 90º

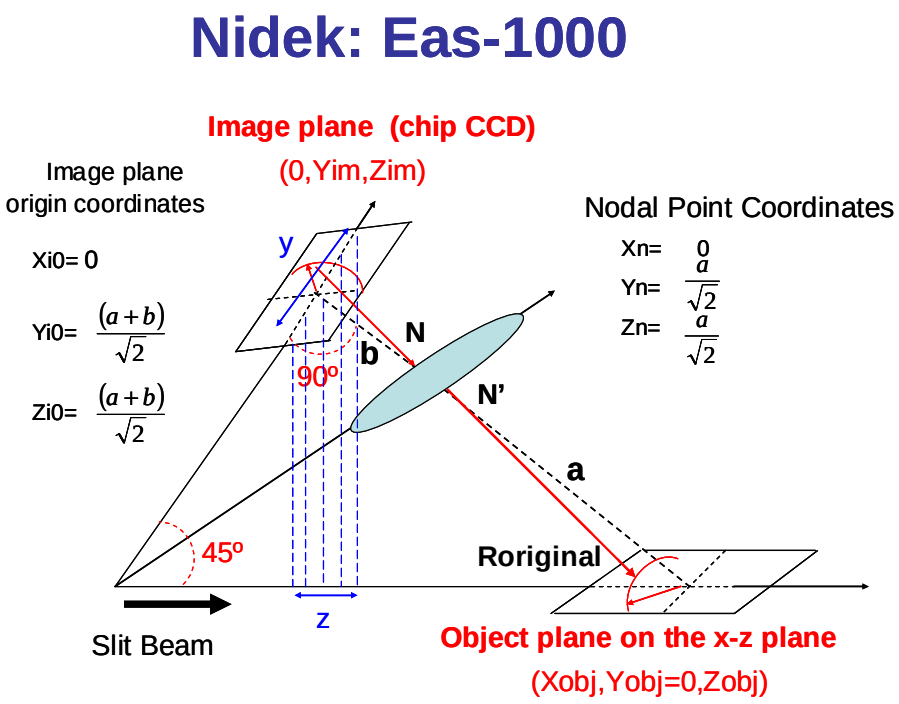

Figure 3.2. Configuration of the Scheimpflug camera Nidek EAS. It can be noticed that the image plane and the object plane form an angle of 45º

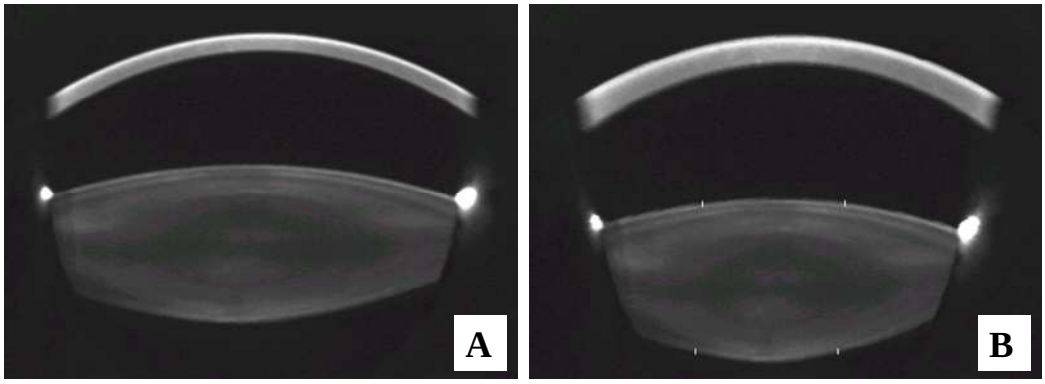

Figure 3.3. Optical and geometrical distortion correction. **A.** Shows a Scheimpflug photo of a 16 years old female before correction. **B.** shows the same photo after correction.

To our knowledge, the only Scheimpflug imaging system commercially available today is the Pentacam system by Oculus. The Pentacam images the anterior segment of the eye by a rotating Scheimpflug camera measurement. This rotating process allows rapid capture of images in different meridians, and therefore three-dimensional elevations.

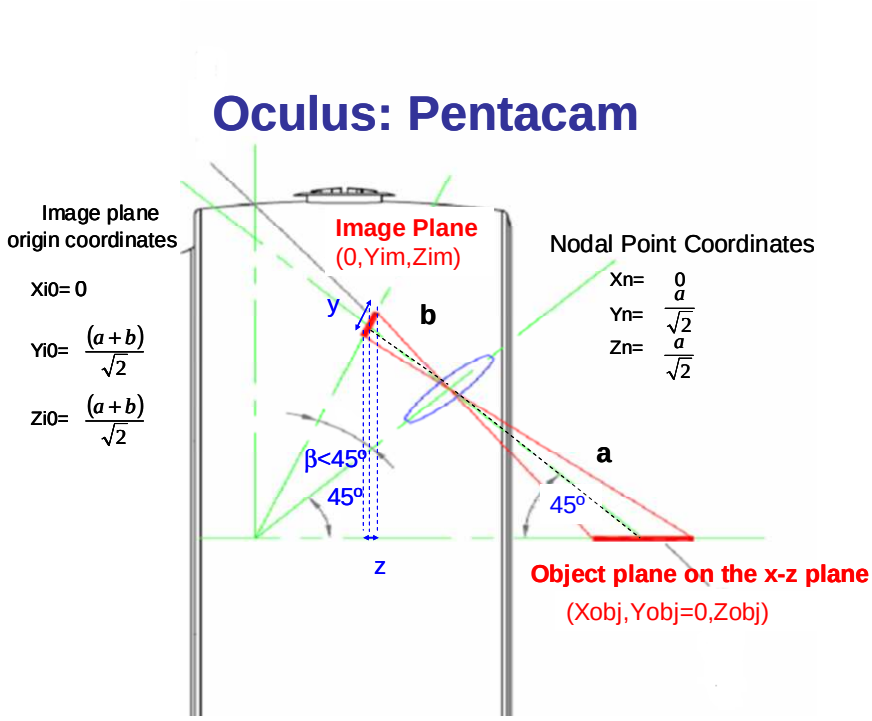

Figure 3.4. Configuration of the Scheimpflug camera Pentacam (Oculus). In this case, the object and image planes form an angle smaller than 90º. This angle was not provided by the manufacturer and it will be an unknown to obtain.

The Pentacam provides optical distortion corrected data of the posteior cornea, although it does not perform any distortion correction on the crystalline lens surfaces.

Figure 3.4 shows the optical layout of the system, as reconstructed from the specifications provided by the manufactured upon request. The Scheimpflug images of Chapter 5 of this thesis were performed using the Pentacam system.

In this Chapter we present the algorithms developed in this thesis for geometrical, and particularly, optical correction of anterior segment images obtained with the Pentacam Scheimpflug system. These algorithms are based on to those developed by Dubbelman for the Topcon and Nidek systems, adapted to the particular configuration of the new system. Since the manufacturer did not provide some critical specifications of the system (CCD pixel size or nodal point distances) additional work was conducted to infer this information.

2. METHODS

In this chapter a method to correct the optical distortion of the Pentacam is proposed.

2.1 Obtaining images from the raw data

The Pentacam stores raw images of the anterior segment of the eye in *.src files. However, the extraction of the raw images from those files is proprietary. An algorithm to obtain original images from the raw data was provided by D. Atchison and S. Kasthurirangan from the School of Optometry, Queensland University of Technology (Australia). The processing algorithms therefore work on the raw images obtained by the system's CCD camera (Oculus, Pentacam).

2.2 Image Processing

Ocular surfaces were detected using a Canny filter in most cases, on images from one single meridian and resulting from an average of 15 identical images. In those images where the lens surfaces were not properly detected using the Canny filter, a manual detection was used instead.

2.3 Obtaining information about the Pentacam's configuration

The application of the correction distortion algorithms requires knowledge of the camera's nodal points and the angle between the image and object plane of the camera (*a, b, angle*), respectively where *a* is the distance between the lens and object planes, and *b* is the distance between the image and the lens planes, those distances give the

nodal point position. However, these parameters have not been provided by the manufacturer.

In order to obtain those values, the following procedure has been followed. Calibrated spheres of known radii of curvature (9.65, 8 and 6 mm) have been placed in different positions along the image plane (Figure 3.4), and imaged with the Scheimpflug system at a given meridian. Ray tracing was recursively performed with varying values of *a*, *b*, and *angle*. A minimization procedure (mean least squares) was applied to obtain the *a*, *b*, and *angle* values that minimized the difference between the estimated and nominal radius of curvature of the calibrated sphere (Figure 3.5). As a proof that the estimated nodal point was correct, a projection of two consecutive points from a millimeter paper was obtained in order to check if the distance between two consecutive points projected was 1 mm. The minimization routine was performed with randomized initial conditions for values of *a* and *b*, with combination of values between 63 and 250 mm, until two conditions were reached:

1) Difference between nominal and obtained radius was 0 mm.
2) Distance between two consecutive points in the millimeter paper was 1 mm.

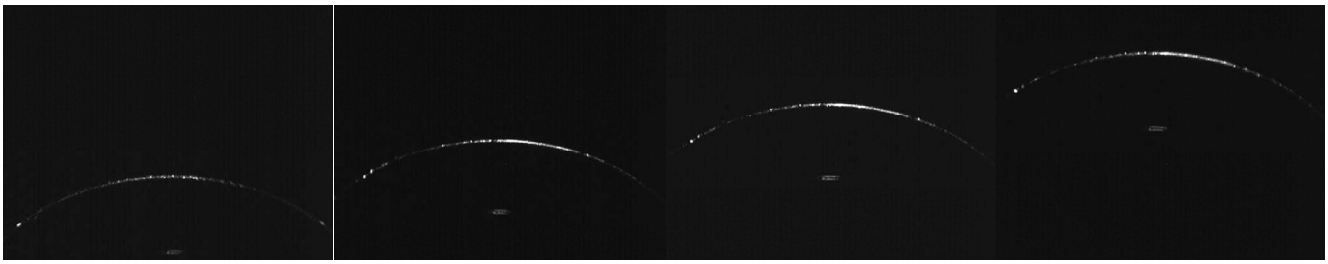

Figure 3.5. Image of the 9.65 mm sphere in different Y positions in the object plane.

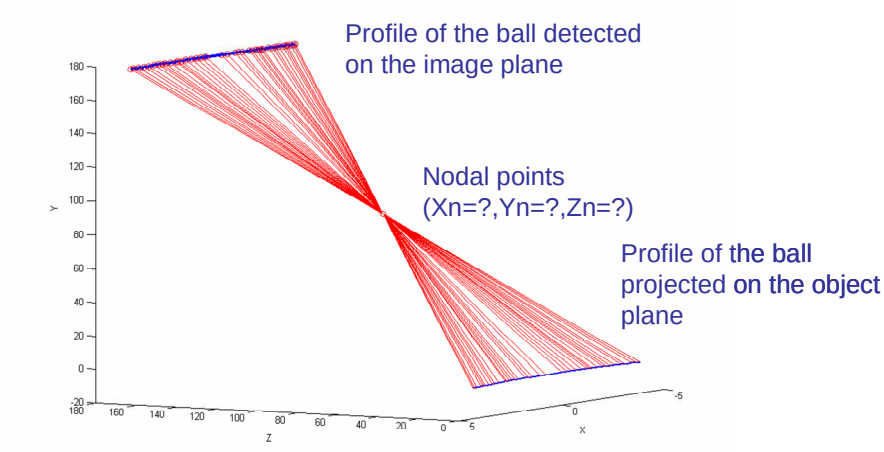

Figure 3.6. Ray tracing back from the image plane to the object plane passing through the nodal points.

2.3. Applying the distortion's correction algorithm

In the ray tracing technique, the slit beam projected on the anterior eye segment is regarded as the object plane, and the CCD- chip as the image plane. The steps followed for the distortion correction are:

a) The anterior surface of the cornea is traced from the image plane, through the nodal points of the camera, to the object plane to obtain its real coordinates.

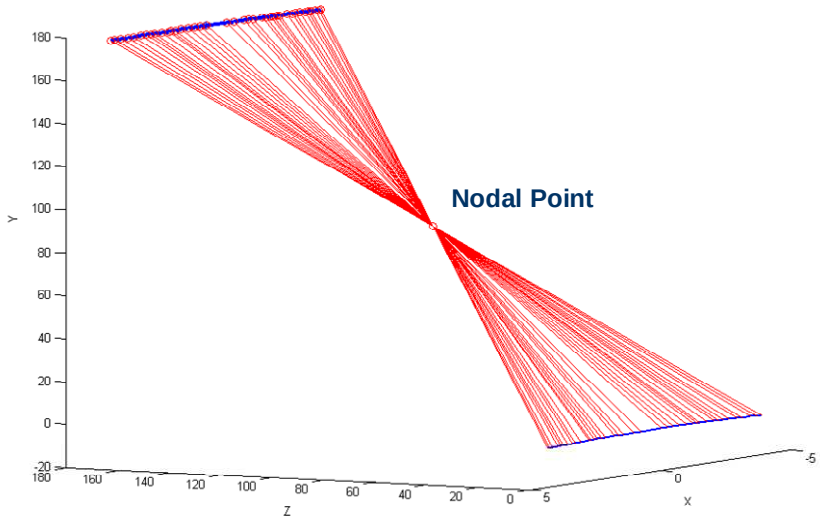

Figure 3.7. Projection of the anterior cornea surface to the object plane passing through the nodal points using a ray tracing procedure.

b) A conic of revolution is fitted to the anterior corneal surface (a sphere in the example).

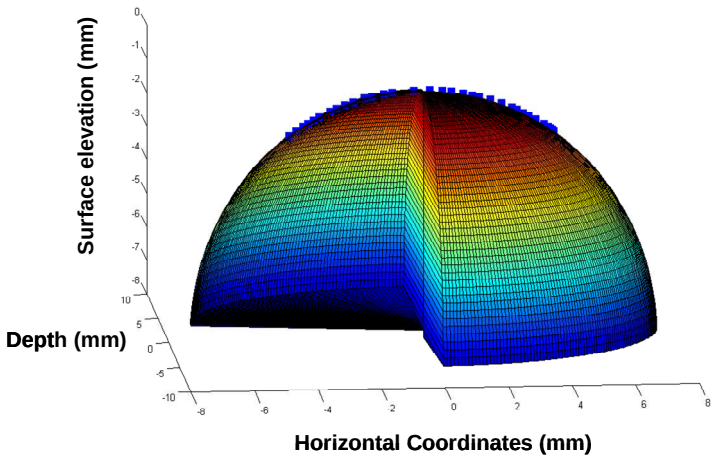

Figure 3.8. The projected points in the object space are fitted to a circle. Considering revolution symmetry, a sphere is raised.

c) Assuming that the surface is rotationally symmetric, the posterior surface is traced from the image plane through the nodal point of the camera and refracted by the anterior cornea, and then projected on the object plane. The projected points are fitted to a conic of revolution (a sphere in the example).

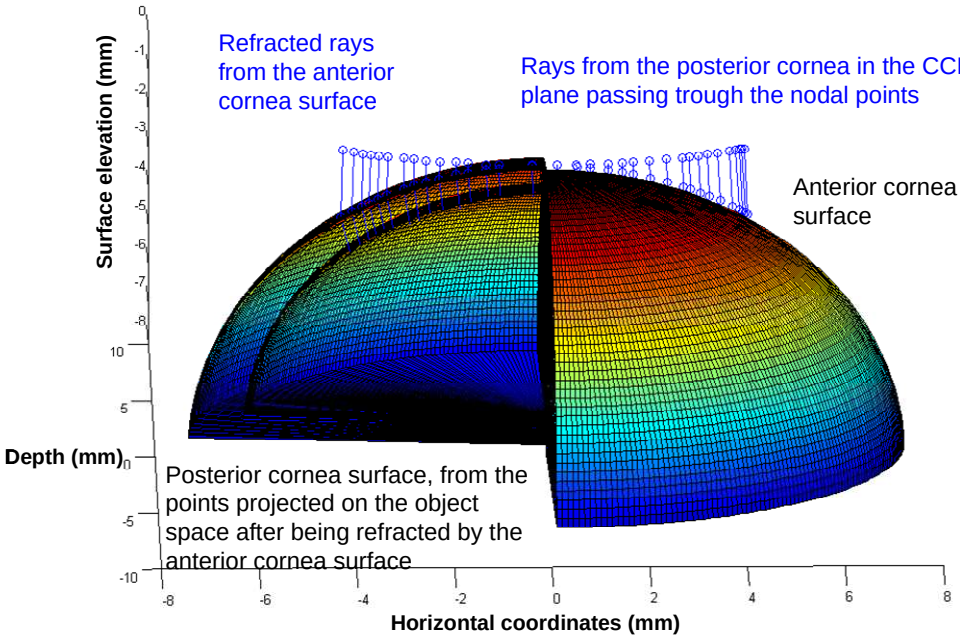

Figure 3.9. The projected points in the object space from the posterior cornea and refracted by the anterior cornea. The surface obtained from the image plane, passing through the nodal points and being refracted by anterior surfaces will be the corrected surface.

d) The same procedure is followed for the anterior and posterior lens surfaces.

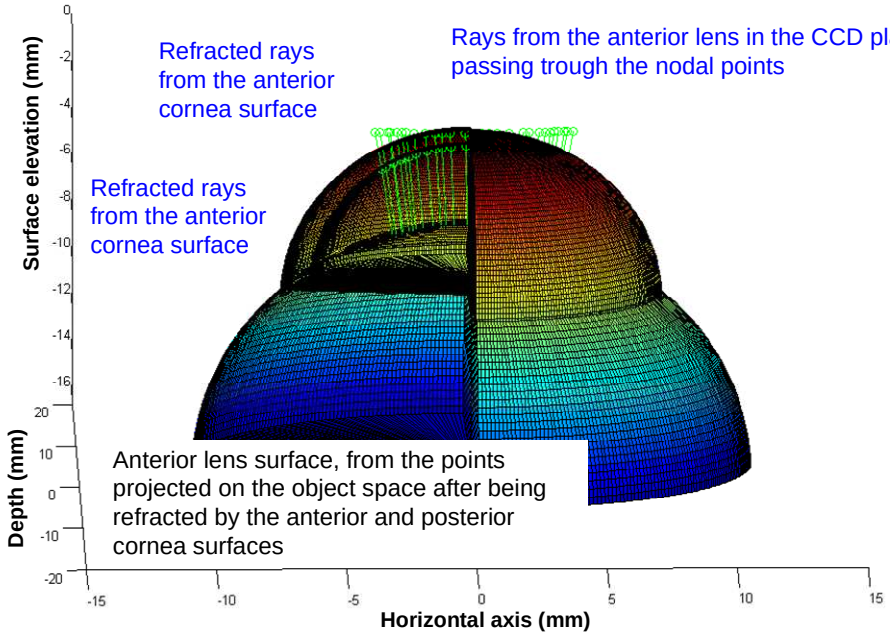

Figure 3.10. The projected points in the object space from the anterior crystalline lens, refracted by the anterior and posterior cornea surfaces.

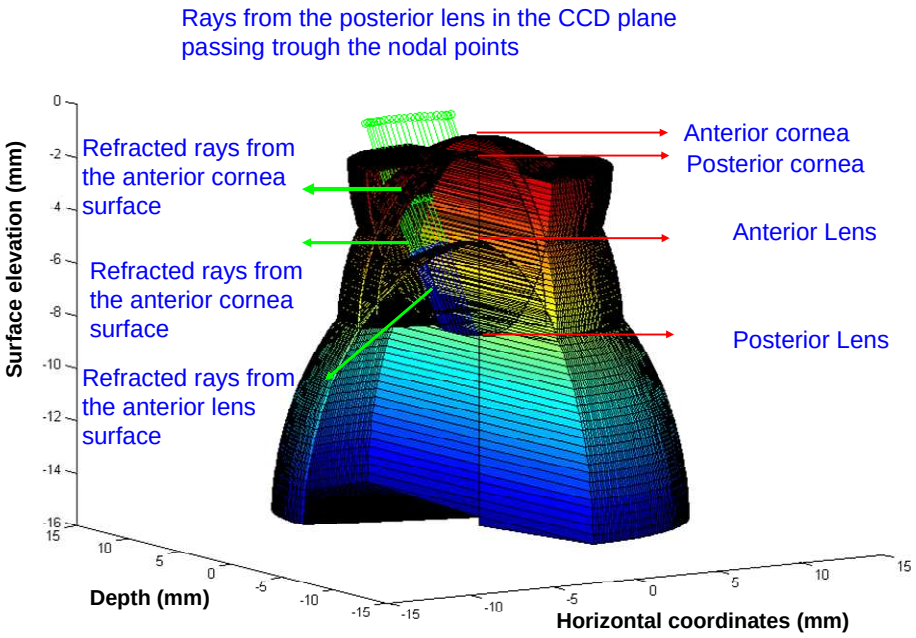

Figure 3.11. The projected points in the object space from the posterior crystalline lens, refracted by the anterior and posterior cornea surfaces and by the anterior crystalline lens

3. RESULTS

3.1 Nodal Points

Using the minimization procedure previously described, the position of the nodal points that reproduces the nominal radii of curvature of the calibrating spheres in the least-squares sense were obtained. The retrieved parameters are: a = 74. 83 and b = 86.09 mm. With those values, radii of curvature of the spheres agreed 100% with the nominal values while the distance between consecutive points in the projected millimetre paper marks was underestimated in 0.05 mm.

3.2 Correction distortion algorithms

In order to estimate the accuracy of the distortion correction algorithms, measurements were performed on an physical model eye and a real human eye. The physical model eye consisted of a PMMA cornea and a spherical intraocular lens (CeeOn, 19D, Pharmacia) (Sverker, Artal, Piers & van der Mooren, 2003), in place of the crystalline lens, with known radii of curvature and known refractive index (Figure 3.12). The normal human eye used as a reference had been previously measured with the distortion corrected Scheimpflug Topcon-SL in the Vrije University, Amsterdam.

Figure 3.13 shows an uncorrected Scheimpflug image obtained with the Nidek EAS-1000 **(A)** and with the Pentacam system **(B)**.

Figure 3.12. Scheimpflug image of an artificial eye of known dimensions (mm).

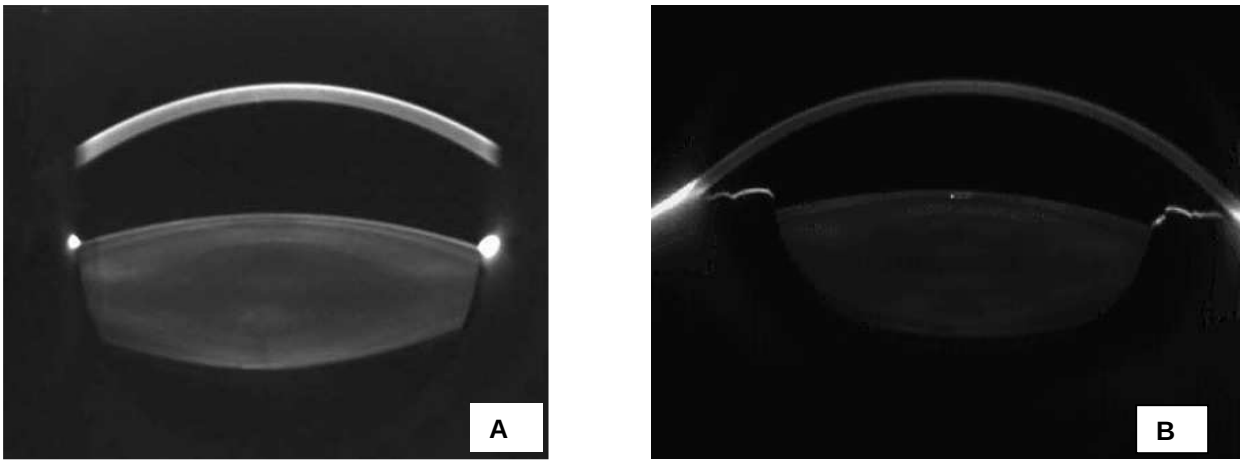

Figure 3.13. A. Distortion uncorrected image obtained with the Nidek EAS-1000 Scheimpflug camera and **B.** Distortion uncorrected image obtained with the Pentacam (Oculus) Scheimpflug camera.

Figure 3.14 shows images of the artificial eye (A) and the normal eye with the uncorrected surfaces detected (blue lines) and the position of the corrected surfaces (B) (red lines) after application of the developed distortion-correction algorithms.

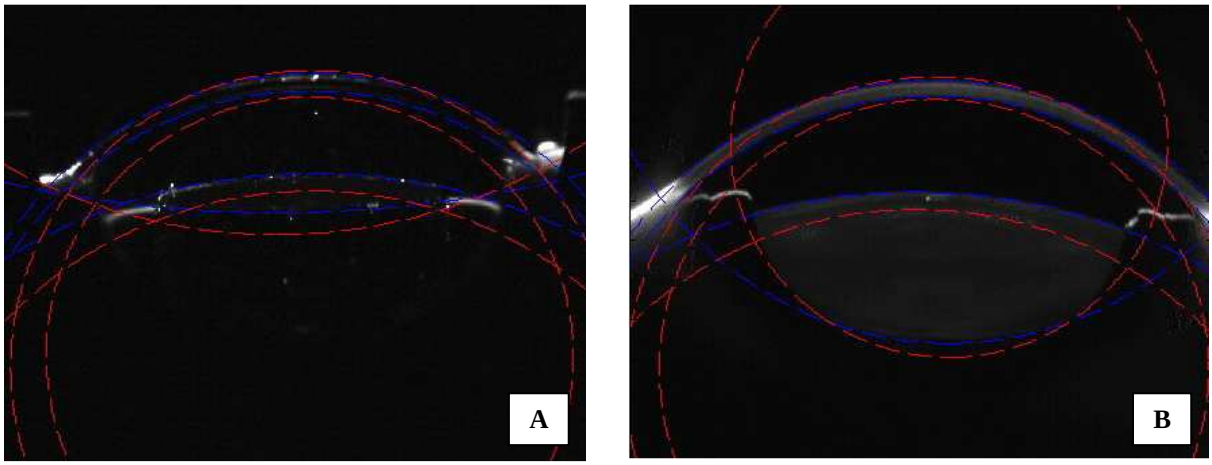

Figure 3.14. Corrected Scheimpflug images. Blue lines represent the detected edges on the uncorrected image. Red lines represent the corrected surfaces for the artificial eye. **A.** Artificial eye. **B.** Normal human eye.

Tables 3.2 and 3.3 show the radii of curvature of the anterior and posterior cornea and anterior and posterior lens and inter ocular distances of the physical and human eye respectively, and those obtained before and after applying the developed distortion correction algorithms for the Pentacam Scheimpflug.

Table 3.2. Radii of curvature of the ocular surfaces and intraocular distances of the artificial eye and the normal human eye before and after distortion correction.

	ARTIFICIAL EYE	NORMAL EYE
Anterior Cornea Radius (mm)	7.8	7.72
Cornea thickness (mm)	0.55	0.54
Posterior cornea radius of curvature (mm)	6.48	6.48
Anterior Chamber Depth (mm)	3	3.15
Anterior Lens Radius of curvature (mm)	12.25	10.54
Lens Thickness (mm)	1.164	4.04
Posterior Lens Radius of curvature (mm)	12.25	5.80

Table 3.3. Radii of curvature of the ocular surfaces and intraocular distances of the artificial eye and the normal human eye

	ARTIFICIAL EYE		NORMAL EYE	
	Before Correction	**After Correction**	**Befote Correction**	**After Correction**
Anterior Cornea Radius of curvature (mm)	8.98	7.59	9.43	7.86
Cornea thickness	0.31	0.53	0.43	0.55
Posterior cornea radius of curvature (mm)	8.48	6.43	8.99	6.97
Anterior Chamber Depth (mm)	2.15	2.52	2.48	2.86
Anterior Lens Radius of curvature (mm)	15.85	11.68	14.68	10.37
Lens Thickness	0.99	1.24	3.83	4.06
Posterior Lens Radius of curvature (mm)	24.26	11.59	8.87	5.55

4. CONCLUSION

We have developed distortion correction algorithms for the Pentacam Scheimplug system. These algorithms have proved to recover the radii of curvature of the different ocular surfaces of a physical model eye, and real eye previously measured with other techniques. Minimization algorithms have been necessary to obtain the location of the nodal points of the camera. The lack of information on the optical parameters of the Pentacam Scheimpflug system has imposed a limitation on the correction algorithms with respect to those developed by other authors for previous Scheimpflug systems.